

**ORIGINAL
RESEARCH**

Y. Kato
S. Higano
H. Tamura
S. Mugikura
A. Umetsu
T. Murata
S. Takahashi

Usefulness of Contrast-Enhanced T1-Weighted Sampling Perfection with Application-Optimized Contrasts by Using Different Flip Angle Evolutions in Detection of Small Brain Metastasis at 3T MR Imaging: Comparison with Magnetization-Prepared Rapid Acquisition of Gradient Echo Imaging

BACKGROUND AND PURPOSE: Early accurate diagnosis of brain metastases is crucial for a patient's prognosis. This study aimed to compare the conspicuity and detectability of small brain metastases between contrast-enhanced 3D fast spin-echo (sampling perfection with application-optimized contrasts by using different flip angle evolutions [SPACE]) and 3D gradient-echo (GE) T1-weighted (magnetization-prepared rapid acquisition of GE [MPRAGE]) images at 3T.

MATERIALS AND METHODS: Sixty-nine consecutive patients with suspected brain metastases were evaluated prospectively by using SPACE and MPRAGE on a 3T MR imaging system. After careful evaluation by 2 experienced neuroradiologists, 92 lesions from 16 patients were selected as brain metastases. We compared the shorter diameter, contrast rate (CR), and contrast-to-noise ratio (CNR) of each lesion. Diagnostic ability was compared by using receiver operating characteristic (ROC) analysis. Ten radiologists (5 neuroradiologists and 5 residents) participated in the reading.

RESULTS: The mean diameter was significantly larger by using SPACE than MPRAGE (mean, 4.5 ± 3.7 versus 4.3 ± 3.7 mm, $P = .0014$). The CR and CNR of SPACE (mean, $57.3 \pm 47.4\%$, 3.0 ± 1.9 , respectively) were significantly higher than those of MPRAGE (mean, $37.9 \pm 41.2\%$, 2.6 ± 2.2 ; $P < .0001$, $P = .04$). The mean area under the ROC curve was significantly larger with SPACE than with MPRAGE (neuroradiologists, 0.99 versus 0.88, $P = .013$; residents, 0.99 versus 0.78, $P = .0001$).

CONCLUSIONS: Lesion detectability was significantly higher on SPACE than on MPRAGE, irrespective of the experience of the reader in neuroradiology. SPACE should be a promising diagnostic technique for assessing brain metastases.

The therapeutic strategies for brain metastases are usually based on a diagnosis using contrast-enhanced MR imaging and depend on the number, size, and location of lesions. In patients with <3 metastatic lesions, aggressive management such as resection or stereotactic radiosurgery is generally recommended.¹ Because the local control rate of brain metastasis by radiosurgery is significantly higher in small lesions (≤ 10 -mm diameter),² early accurate diagnosis of brain metastases by using MR images is crucial for the patient's prognosis.

Several investigators reported that gradient-echo (GE) images usually provide lower contrast enhancement than spin-echo (SE)-type images at 1.5T, though the specific explanation of this phenomenon has not been clearly described.³ This is why the reported detectability of small brain metastases with contrast-enhanced 3D GE images is lower than that with 2D SE images, even if 3D GE sequences, which reduce the partial

volume effect due to acquisition with thinner section thickness, are performed at 1.5T.^{3,4}

Recently, 3T MR imaging units have become widely available for clinical use. Given some disadvantages of 3T units, such as specific absorption rate (SAR) limitations and low contrast between gray and white matter of the brain on T1-weighted SE images, GE techniques that allow lower SAR, higher gray-white contrast, and rapid acquisition of 3D images are generally used for T1-weighted brain imaging at 3T.^{5,6} Furthermore, because the contrast enhancement effect at 3T is higher than that at 1.5T, several studies have suggested that 3D contrast-enhanced GE images provide higher detectability of small brain metastases than 2D contrast-enhanced SE T1-weighted images when a 3T system is used.^{7,8}

Although high SAR at 3T makes it difficult to obtain T1-weighted 3D images with an SE-type sequence, recent technologic innovations, including parallel imaging, k -space trajectory, and variable flip angles, have solved the problem. Sampling perfection with application-optimized contrasts by using different flip angle evolutions (SPACE) is one such 3D SE-type sequence available at 3T. It is a 3D fast SE sequence with variable flip-angle refocusing pulses developed by Mugler et al.⁹ Considering the predominance of contrast enhancement on SE images, we believe the detectability of enhancing lesions on SE images would be higher than that on GE images,

Received October 14, 2008; accepted after revision December 15.

From the Departments of Diagnostic Radiology (Y.K., S.H., S.M., A.U., T.M., S.T.) and Noninvasive Diagnostic Imaging (H.T.), Tohoku University Graduate School of Medicine, Sendai, Japan.

Please address correspondence to Yumiko Kato, MD, Tohoku University Graduate School of Medicine, Diagnostic Radiology, 1-1 Seiryomachi, Aoba-ku, Sendai, Miyagi-ken, 980-8574, Japan; e-mail: ykato@rad.med.tohoku.ac.jp

DOI 10.3174/ajnr.A1506

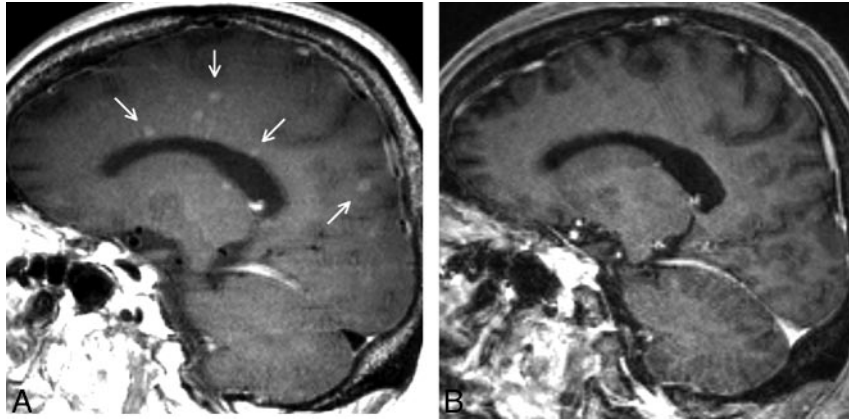


Fig 1. A case with brain metastases depicted clearly on SPACE. *A*, Sagittal image of contrast-enhanced SPACE. *B*, Sagittal image of contrast-enhanced MPRAGE. The anatomic levels of these images conform. The SPACE image shows numerous small enhancing lesions, whereas only a few lesions with subtle enhancement are barely visible on MPRAGE image. Arrows indicate lesions delineated only on SPACE.

given an identical spatial resolution. In our experience with 3T MR images, several metastatic foci were clearly delineated on contrast-enhanced SPACE images, but not on other sequences, including contrast-enhanced 3D GE T1-weighted (magnetization-prepared rapid acquisition of GE [MPRAGE]) images, which were reported to be more helpful than contrast-enhanced 2D SE images to detect small brain metastases at 3T (Fig 1).^{7,8}

In view of the contrast-enhancement effect, we formed a hypothesis that contrast-enhanced SPACE imaging would be more useful than contrast-enhanced MPRAGE in detecting brain metastasis. That was why we compared the conspicuity of brain metastases and the diagnostic performance between contrast-enhanced SPACE and MPRAGE.

Methods and Materials

This study was approved by the local institutional review board and prospectively performed after obtaining informed consent from all patients.

MR Imaging

All studies were performed with a 3T MR imaging system (Magentom Trio a Tim; Siemens, Erlangen, Germany) by using a 12-channel head coil. Contrast-enhanced 3D imaging was performed after injecting the standard dose (0.1 mmol/kg) of gadopentetate dimeglumine (Magnevist; Bayer Schering Pharma, Berlin, Germany) by using the following parameters: TR, 2000 ms; TE, 2.98 ms; imaging time, 4 minutes 50 seconds; FOV, 240 × 256 mm; bandwidth, 240 Hz/pixel; echo spacing, 7.1 ms; and 1-mm-thick sections for MPRAGE; TR, 500 ms; TE, 15 ms; imaging time, 4 minutes 42 seconds; FOV, 240 × 256 mm; bandwidth, 574 Hz/pixel; echo spacing, 5.16 ms; turbo factor, 47; echo trains per section, 4; and 1-mm-thick sections for SPACE. To reduce imaging time, we obtained sagittal 3D planes covering the entire brain with each pulse sequence.

Before obtaining these contrast-enhanced 3D T1-weighted images, conventional T1-weighted (SE, axial), T2-weighted (fast SE, axial), and contrast-enhanced 2D T1-weighted (SE, axial and coronal) images were obtained. To avoid timing bias after contrast injection, we alternated the order of the two 3D sequences (SPACE and MPRAGE) in 69 patients by rotation.¹⁰

Patients

Between August 2007 and January 2008, 69 consecutive patients who were scheduled for examination under 3T MR imaging units for possible brain metastases were imaged prospectively by using 2 types of 3D T1-weighted sequences with contrast enhancement (MPRAGE and SPACE).

From these patients, we selected those with no lesions and those with brain metastases by the following procedures: First, 1 neuroradiologist (Y.K.) reviewed all the contrast-enhanced images of the initial MR imaging (including conventional imaging, SPACE, and MPRAGE) of each patient and divided them into groups with abnormal contrast-enhancing areas (“suspicious lesion”) or with no lesions. In this process, all lesions that were interpreted as having abnormal contrast enhancement among contrast-enhanced sequences (conventional SE, SPACE, and MPRAGE) were selected as suspicious lesions. From the suspicious lesion group, we chose patients who underwent follow-up MR imaging for more than 1 month, because the previous studies reported that shrinkage of brain metastatic foci would be seen in approximately 1 month after treatment.^{11,12} Four cases were discarded due to no follow-up study or an inadequate follow-up period. There were 131 enhancing lesions from 19 patients with follow-up MR images. Then, 2 neuroradiologists (the coordinators, Y.K. and S.M.) determined in consensus fashion whether these 131 suspicious lesions in the selected cases could be considered brain metastases. When a lesion met all the following criteria, the lesion was determined to be a metastasis:

- 1) The “lesion” was not a normal structure or an artifact.
- 2) The lesion was located in the brain parenchyma.
- 3) In addition, the size of the lesion decreased after therapy or increased on follow-up MR images (either MPRAGE or SPACE).

To distinguish normal-enhancing structures, such as vessels or the choroid plexus, and artifacts from lesions, the coordinators carefully evaluated consecutive sections on contrast-enhanced 3D images. Multiplanar reconstructions of the 3D images and other images were used if needed.

Ninety-two enhancing lesions were designated as being brain metastases (follow-up period, 1.5–5 months) and 39 enhancing lesions, as not being brain metastases (follow-up period, 1.5–5 months), including 1 meningioma, 3 meningeal disseminations, 6 vessels, and 29 unchanged lesions. Because this study aimed to check the conspicuity

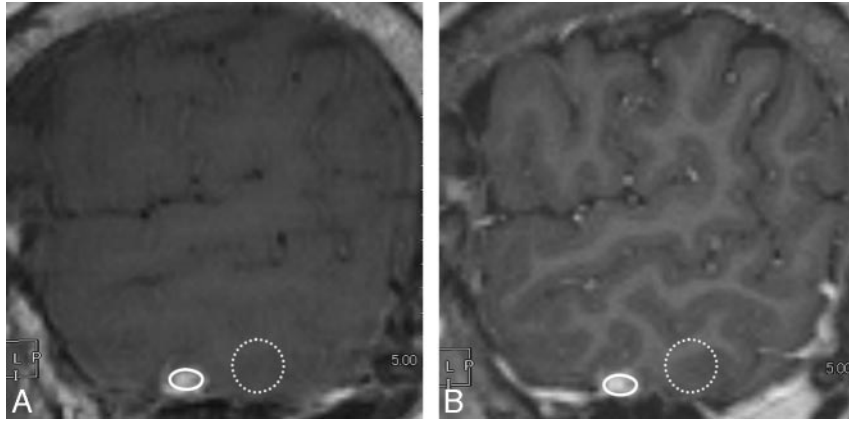


Fig 2. Definition of the regions of interest. *A*, Contrast-enhanced sagittal SPACE image. *B*, Contrast-enhanced sagittal MPRAGE image. A circular or oval region of interest for a lesion is as large as possible, excluding lesion edges, to avoid a partial volume effect (*solid oval*), and the region of interest for the background is on the brain parenchyma near the lesion in the same plane (*dotted circle*). We defined these regions of interest carefully to avoid CSF or vessels. The size and shape of the region of interest on the brain parenchyma are identical on both SPACE and MPRAGE images.

and detectability of brain metastases, these 39 lesions were excluded from the analyses.

Finally, 46 patients (34 men, 12 women; mean age, 63.0 years; range, 36–81 years) were classified as the group with no lesions, and 16 patients (7 men, 9 women; mean age, 57.3 years; range, 42–82 years), as the group with brain metastasis (92 lesions). Thirty-four of the 92 lesions (36%) were depicted with SPACE first, and 58 lesions (63%), with MPRAGE first. The primary tumors of the metastasis group included lung ($n = 11$), breast ($n = 1$), colon ($n = 1$), and pancreatic ($n = 1$) cancer; renal cell carcinoma ($n = 1$); and testicular tumor ($n = 1$). There were 92 brain metastatic foci (49 increased in size, 43 decreased in size).

Image Analysis

The 2 types of contrast-enhanced 3D images were compared by using quantitative and qualitative assessments.

Quantitative Assessments

The measured lesion size, contrast rate, and contrast-to-noise ratio (CNR) were compared between the SPACE and MPRAGE sequences. All these quantitative values were measured on the primary sagittal images by using a stand-alone workstation (Virtual Place Lexus, AZE, Tokyo, Japan).

Size of the Lesions

One neuroradiologist measured the shorter diameter of each lesion in the sagittal plane of both SPACE and MPRAGE images.

Contrast Rate and CNR

The contrast rate and CNR were calculated by using the following formulas. The contrast rate was defined according to Rand et al¹³:

$$\text{Contrast rate} = \{(SI_{\text{lesion}} - SI_{\text{background}})/SI_{\text{background}}\} \times 100,$$

$$\text{CNR} = (SI_{\text{lesion}} - SI_{\text{background}})/SD_{\text{lesion}}$$

where SI_{lesion} and $SI_{\text{background}}$ represent the mean signal intensities of the enhancing lesion and surrounding brain parenchyma, respectively, and SD_{lesion} is the SD of the signal intensity measured for SI_{lesion} . These parameters were obtained by defining regions of interest on images that delineated the greatest dimension of the lesion (Fig 2). The surrounding brain parenchyma for $SI_{\text{background}}$ included

both white and gray matter. Because signal intensities could be changed largely with the balance of white and gray matter in the region of interest, we set a relatively large region of interest for $SI_{\text{background}}$ to reduce the influence: region of interest size of the background on both SPACE and MPRAGE, 76.7 mm² (range, 70–83 ± 2.5 mm²); region of interest size of the lesion on SPACE, 10.7 mm² (range, 1–72 ± 12.9 mm²); region of interest size of the lesion on MPRAGE, 8.1 mm² (range, 1–72 ± 12.5) mm², respectively.

The contrast rate and CNR were measured in 89 and 53 metastatic lesions, respectively. From analysis with the contrast rate, 3 ringlike enhancing lesions were abandoned due to difficulties of setting regions of interest. From analysis with CNR, 36 lesions were abandoned because the region of interest areas were too small to obtain SD values.

Qualitative Evaluation

The diagnostic ability of both sequences was evaluated by using receiver operating characteristic (ROC) analysis. The reading required a set of positive and negative images. For positive images, the coordinators selected those with a single lesion <10 mm in diameter from the brain metastases group because a previous report revealed no difference between contrast-enhanced T1- and T2-weighted images in detecting brain metastases that exceeded 10 mm in diameter.¹⁴ The reason that we selected a single lesion in an image was that multiple lesions in 1 sectional image made it difficult to judge the results. Thirty-six images met the criteria of positive images. Twenty-two of the 36 lesions (61%) were depicted first with SPACE, and the remaining 14 lesions (39%), first with MPRAGE. For negative images, images that corresponded to the aforementioned positive images anatomically but had no metastatic lesion were selected from the no-lesion group. Consequently, 72 images including 36 positive images and the corresponding 36 negative images were selected for the reading. The positive images were chosen from 13 patients (6 men, 7 women), 44–82 years of age (mean, 57.2 years), and the negative images, from 10 patients (5 men, 5 women) 42–76 years of age (mean, 57.8 years). The age difference between the 2 groups was not significant (Student *t* test, $P = .90$).

Ten radiologists, including 5 neuroradiologists other than the coordinators and 5 resident radiologists participated as observers.

The test consisted of 2 series of sessions, 1 each with SPACE and

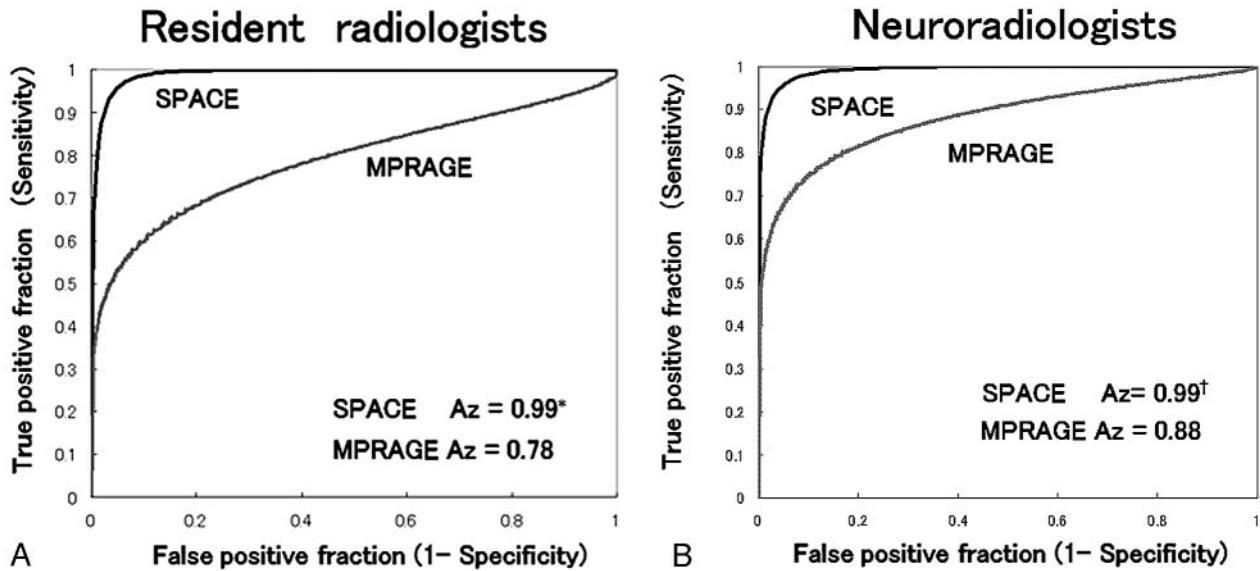


Fig 3. Results of the ROC analyses. In both observer groups, the Az was significantly higher for SPACE than for MPRAGE. The difference in Az values between the 2 observer groups was smaller for SPACE images. The asterisk in *A* indicates residents, $P = .0001$; the dagger in *B*, neuroradiologists, $P = .0013$.

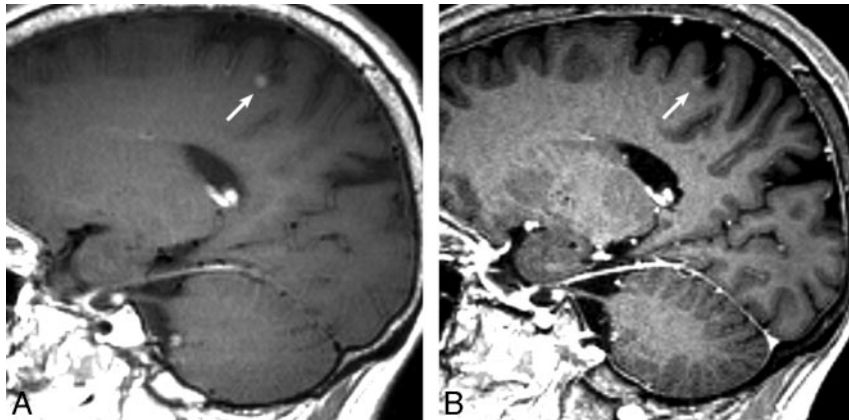


Fig 4. The contrast-enhanced SPACE image (*A*) clearly reveals an enhancing nodular lesion (arrow), whereas the lesion shows faint enhancement on the contrast-enhanced MPRAGE (*B*) and is barely visible. This lesion was noted by 9 observers on SPACE, but overlooked by 8 readers on MPRAGE.

MPRAGE, performed in randomized order under anonymized conditions >4 weeks apart to reduce learning effects. The observers were informed that the purpose of this study was to compare the diagnostic ability of the 2 sequences and that 1 series included 72 images with or without a single metastatic lesion and that the reading time was unlimited. They were blinded to the number of positive images.

Six of the observers (3 neuroradiologists and 3 residents) interpreted the SPACE images first and then the MPRAGE images and vice versa for the other observers. The observers evaluated just 1 section for each case and used the continuous confidence grading scale of a line-marking method. When observers recognized a lesion with a confidence level exceeding 50%, they recorded the most likely position of the brain metastasis on each image. The observers viewed the MR images on a 21.3-inch (54.1-cm) color monitor (CCL250; Totoku Electric Co, Tokyo, Japan) with a display of 1600 × 1200 lines. They were allowed to adjust the image window level and width settings and change the magnification of the images.

Data Analysis

The size, contrast rate, and CNR were compared by using the Wilcoxon signed rank test. Observer performance in detecting brain metastasis was evaluated with ROC analysis by using the observer confidence level. The area under the ROC curve (Az) was calculated by using the computer program LABMRMC.¹⁵ The statistical significance of the difference in the average Az values for both sequences was estimated by using the jackknife method.¹⁶

The observers were required to identify the most likely position of the brain metastasis on each image. True-positive lesions were decided according to brain metastases criteria by the coordinators. Locating true lesions was scored as true-positive events, and all other events were scored as false-positives. The data obtained in this way were used only for determining sensitivity, specificity, accuracy, false-positives, and false-negatives. The differences in the sensitivity, specificity, accuracy, false-positives, and false-negatives were analyzed with a paired *t* test. For all tests used, $P < .05$ was considered statistically significant.

Table 1: Sensitivity and specificity of SPACE and MPRAGE according to the observer groups*

| | Residents | | Neuroradiologists | |
|----------------|--------------------|-------------------|--------------------|-------------------|
| | SPACE | MPRAGE | SPACE | MPRAGE |
| Sensitivity | 96.5† (164/170) | 59.4 (101/170) | 98.8‡ (168/170) | 69.4 (118/170) |
| Specificity | 90 (162/180) | 88.9 (160/180) | 93.3 (168/180) | 90.6 (163/180) |
| Accuracy | 93.1§ (326/350) | 74.6 (261/350) | 96.0¶ (336/350) | 80.3 (281/350) |
| False-positive | 10 (18/180) | 11.1 (20/180) | 6.7 (12/180) | 9.4 (17/180) |
| False-negative | 3.5 (6/170) | 40.6 (69/170) | 1.2# (2/170) | 30.6 (52/170) |

Note:—SPACE indicates sampling perfection with application-optimized contrasts by using different flip angle evolutions; MPRAGE, magnetization-prepared rapid acquisition of gradient echo.

* Data are percentages; numbers in parentheses are raw data.

† $P = .0002$.

‡ $P = .003$.

§ $P = .0008$.

¶ $P = .002$.

|| $P = .0002$.

$P = .01$.

Results

Quantitative Evaluation

Measured Size of the Lesions. The shorter diameters of all the metastatic lesions ($n = 92$) were measured on SPACE and MPRAGE, separately. The measured values were larger by using SPACE than with MPRAGE in 52 lesions (57%), equal in 11 (12%), and smaller in 29 (31%). All the lesions were delineated and measurable on SPACE, whereas 2 lesions were not seen on MPRAGE. The mean diameter measured on SPACE (4.5 ± 3.7 mm; range, 0.7–18.8 mm) was significantly larger than that on MPRAGE (4.3 ± 3.7 mm; range, 0–18.9 mm; Wilcoxon test, $P = .0014$).

Contrast Rate and CNR. The contrast rate was significantly higher on SPACE than on MPRAGE (57.3 ± 47.4 versus 37.9 ± 41.2 ; Wilcoxon test, $P < .0001$). The CNR was significantly higher on SPACE than on MPRAGE (3.0 ± 1.9 versus 2.6 ± 2.2 ; Wilcoxon test, $P = .04$).

Qualitative Evaluation

In 2 cases, several observers noted 2 metastatic lesions on a single positive image. The coordinators re-evaluated these by checking consecutive 3D images and other sequences and determined that both had 2 lesions. These images were excluded from the subsequent analysis. Ultimately, 34 positive images and 36 negative images were analyzed.

For both the neuroradiologists and residents, the diagnostic performance was significantly higher with SPACE images (Figs 3 and 4) and the sensitivity and accuracy were significantly higher on SPACE images (Table 1). The difference in sensitivity between the 2 observer groups was smaller for SPACE images, as was the Az. In contrast, the difference in specificity between them in each observer group was not significant.

Because a previous study revealed no significant difference between 3D and 2D images for detecting enhancing lesions with a diameter of >5 mm,⁷ we compared the sensitivity for lesions <5 and ≥ 5 mm in shorter diameters separately (Tables 2 and 3). On MPRAGE, the detectability decreased

Table 2: Comparison of the sensitivity of the 2 sequences classified by lesion size: results for residents

| Diameter (mm) | Sensitivity with SPACE* | Sensitivity with MPRAGE* | P Value (SPACE vs MPRAGE) |
|------------------------------|-------------------------|--------------------------|---------------------------|
| <5 | 95.7 (110/115) | 50.4 (58/115) | .0001 |
| ≥ 5 | 98.2 (54/55) | 78.2 (43/55) | .011 |
| P value (<5 vs ≥ 5) | .33 | .0005 | |

* Data are percentages; numbers in parentheses are raw data.

Table 3: Comparison of the sensitivity of the 2 sequences classified by lesion size: results for neuroradiologists*

| Diameter (mm) | Sensitivity with SPACE | Sensitivity with MPRAGE | P Value (SPACE vs MPRAGE) |
|------------------------------|------------------------|-------------------------|---------------------------|
| <5 | 98.3 (113/115) | 60.9 (70/115) | .003 |
| ≥ 5 | 100 (55/55) | 87.3 (48/55) | .005 |
| P value (<5 vs ≥ 5) | .18 | .004 | |

* Data are percentages; numbers in parentheses are raw data.

Table 4: Summary of false-positive events*

| False-Positive Events | SPACE (n = 340) | MPRAGE (n = 340) |
|-----------------------|-----------------|------------------|
| Vessels | 8 (5, 3) | 29 (17, 12) |
| Venous sinus | 12 (8, 4) | 1 (1, 0) |
| Choroid plexus | 10 (7, 3) | 1 (1, 0) |
| Infarction | 0 (0, 0) | 1 (0, 1) |
| Artifacts | 4 (2, 2) | 10 (5, 5) |
| Total | 34 (22, 12) | 42 (24, 18) |

* Numbers in parentheses are those of false-positive events that occurred for each observer group (residents, neuroradiologists).

with lesion size and dropped to 50%–60%. In contrast, the deterioration in the detectability of lesions <5 mm in diameter was minimal on SPACE, and their detectability exceeded 95% in both observer groups.

False-positive readings are summarized in Table 4. The total number of false-positive events for all observers was slightly greater with MPRAGE than with SPACE. On MPRAGE, vessels on the brain surface or in the sulci were frequently misinterpreted as metastases. On SPACE, the venous sinuses and choroid plexus in the ventricles tended to be mistaken as lesions. Confusing artifacts included a partial volume effect of the brain cortex and pulsation artifacts from vessels.

Discussion

Lesion Detectability with SPACE and MPRAGE

We compared contrast-enhanced 3D SPACE and MPRAGE images at 3T for detecting small brain metastases with an identical spatial resolution in the same patients. In the reading, the lesion detectability was higher on SPACE than on MPRAGE, and the Az values of the ROC analysis were significantly greater with SPACE images for all observers. The detectability difference between the 2 sequences was more remarkable for smaller lesions (<5 -mm diameter). In addition, the high detection rate on SPACE was insensitive to the observers' experience.

Komada et al¹⁷ compared the detectability of brain metastases on contrast-enhanced images among SPACE, MPRAGE, and 2D SE in a reading with 2 observers. Although they stated

that SPACE might be useful for detecting small brain metastasis, they failed to find a significant difference. Their study did not limit the lesion size and involved only a small number of observers for the reading, all of which might have led to the absence of a significant difference among the sequences.

Presumed Mechanisms for the High Detection Rate on SPACE

The factors contributing to the high detectability of metastatic lesions on SPACE include the higher contrast enhancement effect on SE than on GRE sequences, which is known for 1.5T evaluations.^{3,18} In their 3T study comparing the detectability of small brain metastases (<3 mm diameter), Kakeda et al⁷ reported the superiority of contrast-enhanced 3D GE (3D fast spoiled gradient-recalled [3D SPGR]) images compared with contrast-enhanced 2D SE and contrast-enhanced 2D inversion recovery (IR) images, which they ascribed to the higher signal-intensity-to-noise ratio at 3T and thin sections with 3D acquisition. Nevertheless, they stated that the CNR of metastatic brain lesions on 2D SE was significantly higher than that on 3D GE, also at 3T.⁷

Other studies reported significantly higher contrast between enhancing lesions and normal brain parenchyma on 2D SE than on other sequences, including IR–fast SE, 2D GE, MPRAGE, and fast 3D SPGR at 3T.^{8,19} Komada et al¹⁷ reported that the CNR of brain metastasis on SPACE was significantly higher than that for MPRAGE at 3T. Consistent with them, we found a greater contrast rate and CNR on SPACE, which resulted in the higher contrast enhancement effect on SE than on GE at 3T. Our finding that the metastatic lesions measured significantly larger with SPACE than with MPRAGE may also be explained by the superior contrast rate and CNR of SE sequences (Fig 4).

Another factor producing the high detectability of SPACE involves the magnetization transfer (MT) effect. Because SPACE is based on a fast SE technique, multiple refocus pulses are used. These refocus pulses work as off-resonance ones and provide a greater MT effect in SPACE than in MPRAGE.²⁰ Because the contrast enhancement with gadolinium is related directly to the proton-gadolinium ion interaction, which is not affected by the MT effect, the MT effect preferentially reduces the signal intensity from the brain parenchyma (background). Furthermore, the MT effect suppresses the signal intensity from the white matter to a greater degree, reducing the gray-white contrast. Thus, contrast-enhancing lesions stand out more in the homogeneously suppressed signal intensity of the background (brain parenchyma) on SPACE (Fig 4).

False-Positive Events in the Reading Test

Several false-positive events occurred in both SPACE and MPRAGE, but these confusing pseudolesions differed between the 2 sequences. The superficial vessels were enhanced intensely on MPRAGE, which proved very confusing. In contrast, they were enhanced only modestly on SPACE, as mentioned elsewhere,¹⁷ and this might have contributed to their correct differentiation in our study (Fig 4).

Conversely, venous sinuses and choroid plexuses were often mistaken as lesions on SPACE. This misinterpretation

might have been heightened by the structure of our reading: The observers had to judge whether enhancing structures indicated pathology by evaluating just 1 image section. In a clinical situation, we use a paging method, which enables the observation of consecutive sections of the 3D images, which would improve the diagnostic performance with both SPACE and MPRAGE. This would presumably be even better with SPACE because the choroid plexuses and venous sinuses are sufficiently large enough to be traceable compared with the superficial vessels. The use of multiplanar reconstruction images may also be helpful. Therefore, an even greater diagnostic ability is expected with SPACE in clinical practice. Furthermore, the awareness of confusing structures such as choroid plexuses and venous sinuses would help avoid this kind of misinterpretation.

Potential of the SPACE Sequence

Many studies have reported the utility of double or triple doses of contrast media for detecting small metastatic brain lesions.^{12,21,22} However, nephrogenic systemic fibrosis can occur in some patients with renal failure as a severe side effect of gadolinium contrast medium.²³

Because patients with malignancy may have a variable degree of renal failure with associated chemotherapy, a lower dosage of contrast medium is desirable. We showed that SPACE was excellent for detecting small brain metastases by using a normal contrast dose. Extrapolating from this result, we presume that reducing the dosage of gadolinium contrast may be possible when detecting metastases by using SPACE. However, this needs to be examined further.

Limitations

Our study has several limitations. First, we could not obtain histologic confirmation of the metastatic lesions because patients with multiple brain metastases generally do not undergo surgery. Metastatic foci might be included in the 39 enhancing lesions that were discarded as not being brain metastasis. These lesions would be potentially biased. Nevertheless, we believe that careful observation of 92 lesions, including follow-up imaging studies conducted by 2 neuroradiologists, along with an investigation of the clinical history of malignancy, minimized contamination of our subjects with false-positives and negatives. Second, the regions of interest for some lesions for evaluating the contrast rate were very small (eg, 1 mm²) and corresponded to 1 pixel, which might not have been sufficiently reliable. However, such small regions of interest were unavoidable because this study focused on small metastatic foci. We believe that the excellent result of SPACE in our reading regardless of lesion size supports the validity of the contrast rate.

Finally, the coordinators and readers of the study were not blinded as to which pulse sequence was being evaluated because the gray-white differentiation was so different between SPACE and MPRAGE that they knew the sequence at a glance. This could introduce bias. In conclusion, conspicuity and detectability of brain metastases were better with contrast-enhanced SPACE than with contrast-enhanced MPRAGE.

References

1. Sills AK. **Current treatment approaches to surgery for brain metastases.** *Neurosurgery* 2005;57(5 suppl):S24–32, discussion S1–4
2. Chang EL, Hassenbusch SJ 3rd, Shiu AS, et al. **The role of tumor size in the radiosurgical management of patients with ambiguous brain metastases.** *Neurosurgery* 2003;53:272–80
3. Chappell PM, Pelc NJ, Foo TK, et al. **Comparison of lesion enhancement on spin-echo and gradient-echo images.** *AJNR Am J Neuroradiol* 1994;15:37–44
4. Wenz F, Hess T, Knopp MV, et al. **3D MPRAGE evaluation of lesions in the posterior cranial fossa.** *Magn Reson Imaging* 1994;12:553–58
5. Runge VM, Patel MC, Baumann SS, et al. **T1-weighted imaging of the brain at 3 Tesla using a 2-dimensional spoiled gradient echo technique.** *Invest Radiol* 2006;41:68–75
6. Schwandt W, Kugel H, Bachmann R, et al. **Magnetic resonance imaging protocols for examination of the neurocranium at 3T.** *Eur Radiol* 2003;13:2170–79
7. Kakeda S, Korogi Y, Hiai Y, et al. **Detection of brain metastasis at 3T: comparison among SE, IR-FSE and 3D-GRE sequences.** *Eur Radiol* 2007;17:2345–51
8. Furutani K, Harada M, Mawlan M, et al. **Difference in enhancement between spin echo and 3-dimensional fast spoiled gradient recalled acquisition in steady state magnetic resonance imaging of brain metastasis at 3-T magnetic resonance imaging.** *J Comput Assist Tomogr* 2008;32:313–19
9. Mugler JP 3rd, Bao S, Mulkern RV, et al. **Optimized single-slab three-dimensional spin-echo MR imaging of the brain.** *Radiology* 2000;216:891–99
10. Schörner W, Laniado M, Niendorf HP, et al. **Time dependent changes in image contrast in brain tumors after gadolinium-DTPA.** *AJNR Am J Neuroradiol* 1986;7:1013–20
11. Young RF. **Radiosurgery for the treatment of brain metastases.** *Semin Surg Oncol* 1998;14:70–78
12. Namba Y, Kijima T, Yokota S, et al. **Gefitinib in patients with brain metastases from non-small-cell lung cancer: review of 15 clinical cases.** *Clin Lung Cancer* 2004;6:123–28
13. Rand S, Maravilla KR, Schmiedl U. **Lesion enhancement in radio-frequency spoiled gradient-echo imaging: theory, experimental evaluation, and clinical implications.** *AJNR Am J Neuroradiol* 1994;15:27–35
14. Yuh WT, Tali ET, Nguyen HD, et al. **The effect of contrast dose, imaging time, and lesion size in the MR detection of intracerebral metastasis.** *AJNR Am J Neuroradiol* 1995;16:373–80
15. Kurt Rossmann Laboratories for Radiologic Image Research. The University of Chicago Department of Radiology (2007). ROC SOFTWARE. Available at: http://www-radiology.uchicago.edu/krl/roc_soft6.htm. Accessed February 29, 2008
16. Dorfman DD, Berbaum KS, Metz CE. **Receiver operating characteristic rating analysis: generalization to the population of readers and patients with the jackknife method.** *Invest Radiol* 1992;27:723–31
17. Komada T, Naganawa S, Ogawa H, et al. **Contrast-enhanced MR imaging of metastatic brain tumor at 3 Tesla: utility of T(1)-weighted SPACE compared with 2D spin echo and 3D gradient echo sequence.** *Magn Reson Med Sci* 2008;7:13–21
18. Mugler JP 3rd, Brookeman JR. **Theoretical analysis of gadopentetate dimeglumine enhancement in T1-weighted imaging of the brain: comparison of two-dimensional spin-echo and three-dimensional gradient-echo sequences.** *J Magn Reson Imaging* 1993;3:761–69
19. Fishbach F, Bruhn H, Pech M, et al. **Efficacy of contrast medium use for neuroimaging at 3.0T: utility of IR-FSE compared to other T1-weighted pulse sequences.** *J Comput Assist Tomogr* 2005;29:499–505
20. Constable RT, Anderson AW, Zhong J, et al. **Factors influencing contrast in fast spin-echo MR imaging.** *Magn Reson Imaging* 1992;10:497–511
21. Runge VM, Wells JW, Nelson KL, et al. **MR imaging detection of cerebral metastases with a single injection of high-dose gadoteridol.** *J Magn Reson Imaging* 1994;4:669–73
22. Ba-Ssalamah A, Nobauer-Huhmann IM, Pinker K, et al. **Effect of contrast dose and field strength in the magnetic resonance detection of brain metastases.** *Invest Radiol* 2003;38:415–22
23. Ersoy H, Rybicki FJ. **Biochemical safety profiles of gadolinium-based extracellular contrast agents and nephrogenic systemic fibrosis.** *J Magn Reson Imaging* 2007;26:1190–97